Microchemical Journal 164 (2021) 106087

Contents lists available at ScienceDirect

Microchemical Journal

journal homepage: www.elsevier.com/locate/microc

SO_2- and NO_x- initiated atmospheric degradation of polymeric films: Morphological and chemical changes, influence of relative humidity and inorganic pigments

Laura Pagnin [a,*], Rosalba Calvini [b], Rita Wiesinger [a], Manfred Schreiner [a,c]

[a] Academy of Fine Arts Vienna, Institute of Science and Technology in Art, Schillerplatz 3, 1010 Vienna, Austria
[b] University of Modena and Reggio Emilia, Department of Life Sciences, Via Amendola 2, 42122 Reggio Emilia, Italy
[c] Technische Universität Wien, Institute of Chemical Technologies and Analytics, Getreidemarkt 9/164, 1060 Vienna, Austria

ARTICLE INFO

Keywords:
Polymeric films
Gas ageing and relative humidity
FTIR spectroscopy
Chemical mapping
Principal component analysis (PCA)
Analysis-of-variance-simultaneous component analysis (ASCA)

ABSTRACT

The influence of polluting gases on the stability of polymeric films has not been studied extensively. In fact, the chemical interactions of such materials in contact with the ambient atmosphere depend on different factors such as the environmental conditions, the manufacturing process of the product, the presence of additives or various pigments. In this study, accelerated artificial gas ageing was carried out. The experiments were performed in a gas chamber exposing the samples to sulphur dioxide (SO_2) and nitrogen oxide (NO_x) with a concentration of 15 ppm. The relative humidity (RH) content chosen was 50% and 80% for a total of 168 h of gas exposure. The paint samples under investigation were composed of three different binding media (acrylic, alkyd, and styrene-acrylic) with various inorganic pigments. The morphological changes on the sample surface due to the different impact of the pollutant gases were investigated using a 3D microscope. Moreover, qualitative and semi-quantitative analyses were performed by Fourier-Transform Infrared (ATR-FTIR) spectroscopy, focusing on the degradation reactions and surface mapping evaluation. In order to fully exploit the chemical information on these materials contained in the ATR-FTIR spectra, multivariate analysis was carried out. In particular, Principal Component Analysis (PCA) enabled verifying the main spectral differences between the unaged and aged samples. Moreover, Analysis-of-Variance-Simultaneous Component Analysis (ASCA) was carried out to understand the influence of gas type, relative humidity, and inorganic pigment type on the deterioration process of the binders.

1. Introduction

The knowledge of degradation processes of modern materials, linked to the chemical changes due to the pollutants in the ambient atmosphere, is still of current interest. The outdoor art materials are the most at risk, as the monitoring of environmental parameters, such as humidity, pollutants, or temperature, are not easily controlled and vary according to the different seasonal climatic changes [1]. The atmospheric degradation affects the stability of these materials, and it occurs mainly due to the interaction of the atmospheric constituents including humidity. In fact, water settles in a thin layer on these materials and, acting as a solvent, attracts the pollutants present in the air both gaseous and particulate matter [2]. The main gaseous air pollutants include sulphur dioxide (SO_2), nitrogen oxides (NO_x), ozone (O_3), and particulate matter (PM). The latter two were not considered in this study, however, they also significantly affect artworks. Ozone, being present at high levels in urban areas, is one of the most oxidising pollutants found in nature. Its effect on artwork, combined with sunlight, oxygen, and other pollutants, was tested on different art materials such as watercolours [3], metals, stones, and polymeric binders [4], showing different interactions and physical–chemical reactions depending on the material. A similar deteriorating influence was also evaluated for atmospheric particulate matter [5]. However, being composed of a mixture of solid and liquid particles suspended in the air, and having particles that vary in size and composition, its deteriorating effect changes depending on the art material [6].

SO_2 and NO_x, as reported in the literature [7], have different characteristics: SO_2 is released from the combustion of fossil fuels and the metal refining process, resulting in one of the most important polluting gases present in the atmosphere, whereas, NO_x is produced from both

* Corresponding author.
E-mail address: l.pagnin@akbild.ac.at (L. Pagnin).

https://doi.org/10.1016/j.microc.2021.106087
Received 26 November 2020; Received in revised form 10 February 2021; Accepted 11 February 2021
Available online 17 February 2021

natural and anthropogenic sources, but also the combustion processes. Generally, in the air, it contributes to the formation of other air pollutants and, combined with SO_2, forms the so-called acid rain. Although the concentration of these gases in the air has slowly been decreasing over the last decades, their oxidizing effects affected the early 20th century and older artworks. Studies on different artworks such as stone materials [8] and metals [9] exposed to outdoor environmental agents confirm the presence of sulphates and nitrates on the surfaces. They caused multiple degradation effects as morphological deformations and dry corrosive deposits that, once in contact with water (as rain or high humidity) can dissolve penetrating into the material and causing aesthetic and mechanical damages. While many studies focus on the influence of those gases on traditional art materials [10], the knowledge of the interaction of modern synthetic polymers with those gases is still rudimentary. Some artificial gas ageing studies were already carried out by testing materials similar to those under investigation, but including a stone or metal ground [11–14]. However, the experimental setup presented in this study combined with innovative chemometric methods represents an interesting analytical approach for the evaluation of the chemical behaviour that each polymeric binder develops when exposed to different gaseous pollutants. Moreover, their investigation can be of support for the storage and display practices of artworks in museum environments. Their concentration levels require continuous monitoring to allow an adequate prevention action of more sensitive artistic objects [15].

In this study, the impact of SO_2 and NO_x on the degradation behaviour of modern synthetic polymers was investigated. Alkyd resins, acrylics, and styrene-acrylic emulsions, represent the principal organic binding media used in modern and contemporary art, mainly used in the 20th century but also recently applied in the field of conservation-restoration. Alkyd resins became the modern substitutes of traditional oil painting due to their low-costs, fast-drying, the possibility to employ it with a great variety of pigments, and its excellent optical properties [16]. However, acrylic emulsions became the most common and versatile polymer. Initially, it was used in industry as a plastic material for structural applications. Subsequently, it was possible to develop a more flexible and transparent polymer due to the possibility to add two or more acrylic monomers within the same polymer chain. Its stability, excellent mechanical properties, and rapid drying have made it attractive for artists too. The application and use of these two binders expanded into various other sectors such as coatings for furniture and architectural, product finishes, or for special coatings in the automotive sector. Furthermore, their chemical-physical properties make them suitable for the protection of various materials such as metals, wood, or other plastics from corrosive agents [17].

During the last years of technological development, monomers were added to the acrylic emulsions in order to lower the production costs and to improve its chemical-physical performances, creating new synthetic binders such as styrene-acrylic emulsions. In recent years, this synthetic polymer was widely applied in the coating industry as well as in the artistic field, especially for spray paints and contemporary murals [18]. To study the different influence that gas pollutants have on the degradation of polymers, an accelerated gas ageing study was performed, using synthetic air containing sulphur dioxide (SO_2) and nitrogen oxide (NO_x) combined with different relative humidity (RH%) contents for a total exposure period of 168 h. The samples under investigation were paint mixtures of three different binding media (acrylic, alkyd, and styrene-acrylic) in mixture with nine inorganic pigments. These pigments were chosen because still present in formulations of paint tubes, and their employment is documented also in previous centuries. Therefore, being present both in recent contemporary artworks and in modern ones (since 1800), it is important to study their effects for the long-term stability of artworks [19–22]. The study focused on the application of 3D microscope and ATR-FTIR analysis to investigate degradation products according to the different gas and RH employed. This investigation allowed understanding which binder is more prone to degradation due to gas exposure and which inorganic pigment increases or decreases this effect.

Multivariate statistical analysis of spectroscopic data is becoming an established tool in the field of cultural heritage studies thanks to the ability of these methods to extract the useful information from the analysed data and to find patterns in the spectral response related to the phenomena under investigation [23–26]. In the conservation of cultural heritage, the combination of spectroscopic techniques and chemometrics allows to monitor in a non-destructive manner the deterioration processes of the analysed samples and to gain a comprehensive evaluation of the modifications occurring during degradation [27,28]. This information can be further exploited for age estimation of artworks or to select the proper pigments to be used to artwork restoration [29,30].

For these reasons, in this study multivariate data analysis of the FTIR spectra based on Principal Component Analysis (PCA) and Analysis-of-Variance-Simultaneous Component Analysis (ASCA) were performed to support the chemical information obtained from the FTIR mapping and enabled verifying spectral differences between unaged and aged samples, as well as evaluating the influence of pollutant gases, relative humidity, and inorganic pigments. Having a general overview of the chemical-physical reactions occurring during the surface degradation of materials, it is essential to develop and apply new strategies that can monitor and prevent future deterioration processes.

2. Materials and methods

2.1. Sample preparation

Different samples were prepared by mixing pure acrylic emulsion Plextol® D498 (Kremer Pigmente, Germany), Alkyd Medium 4 (Lukas®, Germany), and styrene-acrylic binder Acronal S790 (BASF, Germany) in combination with 9 inorganic pigments (Kremer Pigmente, Germany). The pigment/binder (P/BM) ratio chosen was 1:3 in weight according to commercial formulations, which guarantee a homogenous mixture with optimum consistency and colourfulness. After mixing them with a ceramic mortar, the fresh paints were cast on glass slides with a film thickness of 150 μm using the so-called Doctor-Blade procedure [31]. The samples were dried at ambient conditions (approx. 22 °C and 30% RH) for three weeks. Mock-ups with pure binders were also prepared (150 paint samples in total). The paint materials investigated are listed in Table 1.

Table 1
List of materials analysed.

Pigments	Chemical composition	Colour Index (C.I.) number
Titanium white	TiO_2	PW6
Cadmium yellow	CdS	PY37
Cobalt green	Co_2TiO_4	PG50
Hydrated chromium oxide green	$Cr_2O_3{\cdot}2H_2O$	PG18
Cobalt blue	$CoO{\cdot}Al_2O_3$	PB28
Cerulean blue	$CoSnO_3$	PB35
Artificial ultramarine blue	$Na_{8\text{-}10}Al_6Si_6O_{29}S_{2\text{-}4}$	PB29
Iron oxide red	Fe_2O_3	PR101
Manganese violet	$NH_4MnP_2O_7$	PV16
Binders	**Chemical composition**	**Commercial Name**
Acrylic emulsion (Alk)	p(nBA/MMA)	Plextol® D498
Alkyd resin (Acr)	Polymer oil-modified polyester-resin	Alkyd Medium 4
Styrene-acrylic emulsion (Sty)	Styrene acrylate copolymer	Acronal® S790

2.2. Weathering experiments

The weathering system used for the atmospheric exposure experiments consists of two parts: the system for mixing synthetic air with corrosive gases [32], and the weathering chamber for gas exposure. To generate the desired concentration of corrosive gases, synthetic air 5.0 (Messer, Austria) is humidified using double-distilled water and mixed with the selected gas. The chamber is continuously flushed with the gas mixture with a gas flow rate of 100 L/h. The chamber (Bel-Art™SP Scienceware™) is made of a co-polyester glass (Purastar®) including gas in- and outlets with a total volume of 30 cm^3. The samples were aged for 168 h. The relative humidity (RH) content chosen was 50 and 80%, whereas the gas concentration selected was 15 ppm both for SO_2 and NO_x. The gas concentration was monitored daily during the artificial ageing using a specific gas sensor for SO_2 and NO_x detection (Aeroqual Limited, New Zealand, model AQL S200). During the ageing experiments, the value could vary by ± 1–0.5 ppm. The values of the gas concentrations were selected in order to reproduce an artificial outdoor ageing. In fact, according to European Environmental Agency for the air quality monitoring, the annual mean concentration of SO_2 in the atmosphere is between 5 and 20 ppb, whereas of NO_x is between 10 and 45 ppb [33]. Converting the experimental gas concentration used in the experiment, the corresponding yearly value is 288 ppb. Therefore, from the annual experimental concentration value and those monitored as average mean in the atmosphere, the exposure time resulting from the artificial accelerated ageing carried out is equal to a value between 10 and 15 years. The RH% values were chosen according to the yearly outdoor weathering changes and to reproduce extreme situations in case of inappropriate museum preventions.

It has to be highlighted that the degradation reactions occurring during natural aging may differ from the degradation process induced by accelerated aging, as reported in several studies [13,34]. However, studies based on accelerated aging represent a necessary step in the preliminary evaluation of degradation processes occurring on artwork materials due to specific pollutants. Indeed, accelerated aging studies allow to monitor the degradation process under controlled conditions and in relatively short times compared to long-term natural degradation.

2.3. Optical 3D Microscope

Each sample was scanned by using the Keyence VHX-6000 microscope (Keyence, Japan). Three-dimensional morphological images were recorded using a VH-Z100 objective (magnification of 1000x). The microscope is equipped with a LED light source (5700 K). To obtain a complete and accurate evaluation of the superficial changes, two different lighting angles were selected. First, the full light ring was used for observations in the dark field and subsequently, the mix light beam (full ring and full coaxial) to emphasize height differences as scratches. To obtain the roughness depth profile of the surface, the total depth obtained is of 10 μm taking a picture every 2 μm (pitch scans).

2.4. Attenuated total reflection fourier transform infrared spectroscopy (ATR-FTIR)

For the ATR-FTIR investigations, a LUMOS FTIR Microscope (Bruker Optics, Germany) in ATR mode with a germanium crystal was employed. The instrument is equipped with a photoconductive cooled MCT detector. Five measuring spots for each sample were acquired in a spectral range between 4000 and 480 cm^{-1} performing 64 scans at a resolution of 4 cm^{-1}. The resulting spectra were collected and evaluated by the software OPUS® (Bruker Optics, Germany). Subsequently, the spectra were averaged, baseline corrected and vector normalized. From the treated spectra, the semi-quantification of selected bands was carried out. As shown in a previous study [35], the chosen integrated bands are the most characteristic of each material and show a significant change in the relative intensity depending on different weathering. In Table S1, the integrated bands divided according to the paint mixtures are listed. For the chemical mapping, the total mapped area had a dimension of 1.0 × 1.5 mm^2; six measuring spots along the x-axis (optical aperture approx. 0.2 mm) and six spots along the y-axis (optical aperture approx. 0.1 mm) have been collected for a total of 36 spots. Each chemical mapping experiment was carried out in three different areas of the samples.

2.5. Chemometrics methods

In the present study, the ATR-FTIR spectra of the paint samples were evaluated by a multivariate statistical approach in order to study the influence of the different experimental conditions on binder degradation [36,37]. Firstly, PCA was applied to gain a preliminary overview of the main differences between unaged and aged samples. Then, ASCA was used in order to systematically assess the effect of pigment type and weathering conditions on the aged samples [38,39]. Both PCA and ASCA were applied to the ATR-FTIR spectra taking into account only the range between 3030 cm^{-1} and 1500 cm^{-1}. This specific spectral range was selected as it only includes the absorption bands ascribable to the considered binders, excluding the spectral regions related to the pigments. The ATR-FTIR spectra were averaged, baseline corrected, and normalized. Before calculating PCA and ASCA models, the spectra were pre-processed using Savitzky-Golay smoothing [40] and mean centering. In the present study, PCA was performed using Chemometric Agile Tool (CAT) software [41] running under R environment (v. 3.1.0). ASCA models were calculated using PLS_Toolbox software (v. 8.5, Eigenvector Research Inc., USA) running under MATLAB environment (R2017b, The MathWorks, USA). Further details about the considered multivariate methods can be found in Supporting Information.

3. Results and discussion

3.1. Optical 3D microscopy

The 3D pictures of each paint sample show the morphological changes and the degradation products appearing after the artificial gas ageing. On pure samples of alkyd and styrene-acrylic binder, no visible morphological changes on the surfaces can be observed, whereas on the pure acrylic sample degradation phenomena are visible after SO_2 and NO_x ageing at 50% RH. Increasing the relative humidity value to 80%, they completely cover the entire polymeric surface making it opaquer. However, a morphological difference between the corrosion products is observed. In fact, depending on the type of gas used, these products deriving from ageing have a different shape (Fig. S1). After NO_x exposure, they are large, broad (radial), surrounded by other smaller ones. On the contrary, after SO_2 exposure, they have a more uniform and compact shape, of a smaller size compared to NO_x ageing. The roughness evaluation obtained from the 3D depth profile confirms that on the sample aged with SO_2, they reach a size between 10 and 15 μm, while after NO_x ageing, the larger ones reach a diameter of 100 μm and the smaller ones between 20 and 30 μm. This behaviour is due to the different interaction that the binder shows according to the type of pollutant gas. However, further analyses are needed to obtain a complete knowledge of this behaviour. The degradation products can be attributed to the surfactant (possibly polyethylene oxide, see chapter ATR-FTIR results) present in the acrylic binder. In fact, having a hygroscopic nature, it tends to migrate to the surface when exposed to high relative humidity values. To confirm its presence, a solubility test was performed [42].

The swab-rolling cleaning test was carried out using distilled water and applied on the surface for a total of 10 s. The surfactant present on the surface of the sample aged with SO_2 were removed, and the surface morphological condition appeared similar to the original one (Fig. 1a). However, those present on the sample aged with NO_x (Fig. 1b) were not completely removed by the action of water. This behaviour is confirmed

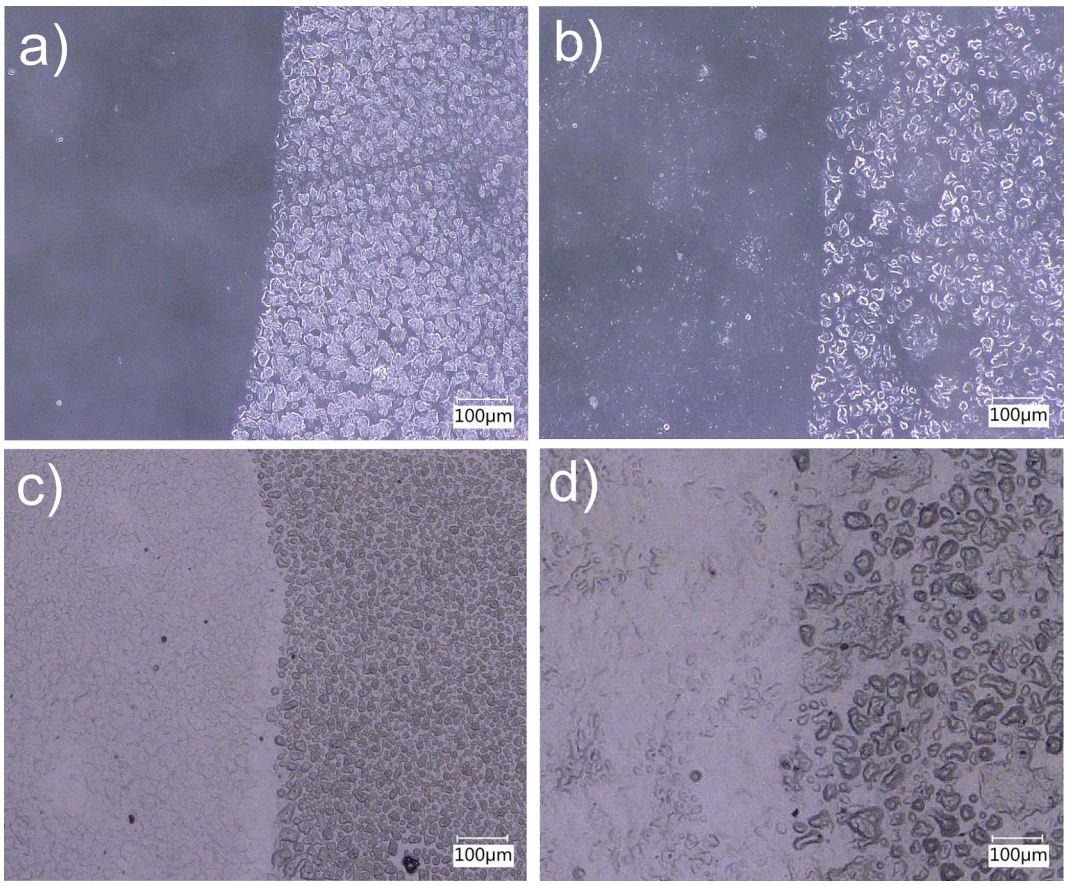

Fig. 1. Overview of the cleaning test results on degraded pure acrylic samples. The images a) and c) show the acrylic surface aged with SO_2 before and after cleaning, whereas, the images b) and d) depict the acrylic surface aged with NO_x. For the top images, the full ring lighting was used, for the bottom images; the mixed lighting was applied.

by observations using the mix light beam (Fig. 1c-d). Furthermore, from the observation of their roughness vertical profiles (Fig. S2a.1-b.1), NO_x ageing had the strongest oxidative effects since the difference between the clean and the aged area is higher than that of SO_2 ageing. In support of this evaluation, a comparison between their horizontal profiles was performed (Fig. S2a.2-b.2). By overlapping the roughness profiles (Table 2), it is observed that the cleaning action had a better result on the surface aged with SO_2 compared to NO_x. In fact, in the latter, the surfactant is still present in some parts (blue areas), probably since the depth of the surfactant particles migrated on the surface of the polymer is more significant and then hard to remove (red areas). Another factor that influences the different degradation effects is the presence of different inorganic pigments in the mixture. In Fig. S3, it can be observed how the degradation effect caused by NO_x exposure is favoured for pigments as PW6, showing evident superficial variations. For pigments such as PB28 and PB29, these effects can only be observed after SO_2 ageing. The same behaviour is observed for alkyd paints (Fig. S4). In this case, the surfaces show the presence of micro-pores after gas ageing (the sizes vary according to the pigment in the mixture) which tend to be more numerous after SO_2 ageing. Finally, styrene-acrylic paints depict the presence of small surface cracks after the exposure to both pollutant gases. In this case, the two different gases cause similar morphological changes and even the various inorganic pigments used do not show a different superficial degradation effect.

Table 2
Morphological values acquired after 3D depth profile evaluation.

	RH %	Gas	Size PEO migrated on the surface after gas ageing	3D depth profile before cleaning	3D depth profile after cleaning
Acrylic film	80	SO_2	10–15 µm	9.38 µm	5.88 µm
	80	NO_x	20–30 µm	10.58 µm	8.84 µm

3.2. ATR-FTIR results

The main functional bands of each paint sample were identified by the use of ATR-FTIR analysis and listed in Table S2. Concerning the acrylic emulsion, ATR-FTIR analysis provided characteristic signals of nBA/MMA copolymer, as identified primarily by the C—H bond stretching vibrations (2956–2876 cm^{-1}), the C═O stretching (1726 cm^{-1}) and the additional bands of the C—O—C and C—O stretching (1236, 1160, 1146 cm^{-1}). Furthermore, PEO (polyethylene ox-ide) surfactant bands are present at 2895, 1343, and 1115 cm^{-1} [35,43]. Observing Fig. 2a–d, it is possible to notice that, in all the acrylic samples aged both with NO_x and SO_2, the intensity of the functional groups increases. It is related to the increase of humidity levels (50–80 RH %) which allow the polymeric structure to gradually open. This behaviour is favoured by the absorption of water by hygroscopic materials inside the paint (in this case the non-ionic surfactant PEO), which can exist in isolated pockets inside the films or can be diffused in the polymer [44]. Consequently, also the spectral signals of the surfactant increase and are higher with increasing the RH content. As reported in the literature [45], the hygroscopicity and solubility of this surfactant promote the migration to the air-film interface. Its accumulation at the interface may affect the mechanical strength of acrylic paints, such as the adhesion of the film to the support, its permeability, surface gloss, and exposure to dirt [46]. However, depending on the type of gas used, the amount of the surfactant on the surface is different. In fact, by exposure of the samples

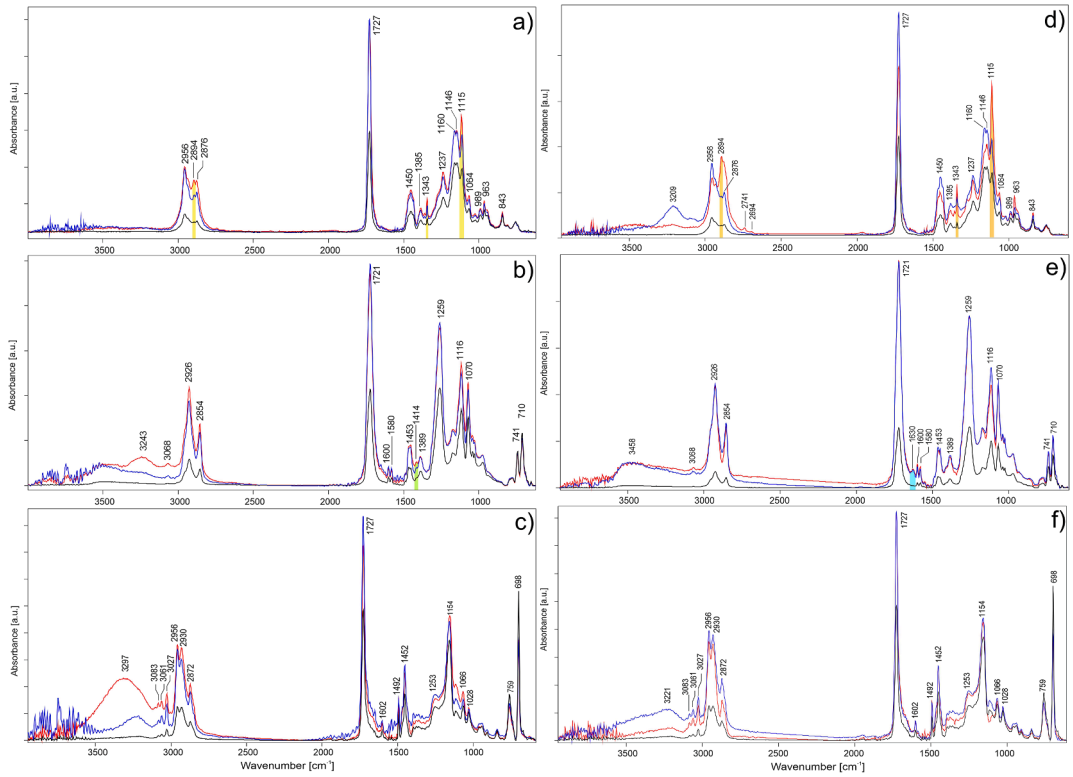

Fig. 2. ATR-FTIR spectra comparison of pure binders: a) and d) acrylic emulsion; b) and e) alkyd resin; c) and f) styrene-acrylic binder. The samples on the left were aged with SO_2, and on the right with NO_x. In each graph, the unaged (black), the 50% RH (blue), and the 80% RH (red) aged samples are showed.

to NO_x, the absorbance signals of PEO increase more than those aged with SO_2. This behaviour is due to the properties of both the binder and the gas. NO_x is more reactive as an oxidative agent than SO_2 [47], and its radicals can abstract the hydrogen atoms from the less strong C—H bonds or interact with the C=C bonds of the macromolecules, initiating the degradation of free radical polymers at room temperature [48]. It may be related to the formation of the bands at 2741–2694 cm^{-1} associated with the overtone of the aldehyde bond. This behaviour, combined with the possibility of the surfactant to form hydrophilic moieties with water, facilitates the migration of PEO to the surface and the hydrolyzation of the binder. The ATR-FTIR analysis per-formed on alkyd paints allows the identification of the most characteristic bands, as shown in Table S2 [49]. The strong band at 1721 cm^{-1} is due to the C=O stretching vibration, common to both oil and phthalate component, whereas the C—O—C stretching (1259 and 1116 cm^{-1}) and the aromatic in-plane and out-of-plane bending (1600–1580, 1070, and 740–710 cm^{-1}) are typical for phthalate structures. Relative to the oil portion, the CH_2 and CH_3 symmetric and asymmetric stretching and bending are assigned [26]. As shown in Fig. 2b–e, also in this case, the intensity of the bands of the alkyd binder tends to increase with the increase of relative humidity, for both gas ageing. This spectral behaviour indicates a hydrolytic degradation of the binder, attributed to the sensitivity to water of *ortho*-phthalate esters in acidic conditions. It is confirmed by the relative decrease in the phthalate group (741–710 cm^{-1}) and by the broadening of the carbonyl band C=O, due to the formation of new oxidized products during the artificial ageing cycles. Therefore, for alkyd paint, the hydrolysis of the phthalate fractions is the main degradation process which also leads to the loss of physical properties of the top layer [50]. Furthermore, two degradation products are observed because of gaseous ageing. From SO_2 exposure, a small band at 1414 cm^{-1} is shown, indicating the formation of the SO-CH_3 bond. According to Simendinger and Balk [51], SO_2 interacts mainly with the drying oil leading to the formation of cross bonds of sulphate esters between the drying oil molecules. This phenomenon is also stimulated by the propensity of fatty acids to be more reactive with SO_2, leading to oxidation reactions. Contrary to these results, a small band at 1630 cm^{-1} is observed for NO_x, related to the formation of the -O-NO_2 bond [52]. As previously mentioned for the acrylic binder, the high relative humidity leads to hydrolytic degradation which, interacting with the gas, forms this bond with the binder. This band is more visible in alkyd paints because favoured by the high reactivity of fatty acids to interact with the gas. Finally, in Fig. 2c-f, the main functional groups of the styrene-acrylic polymer can be identified. Related to the acrylate part, the C—H bond stretching vibrations (2956–2930–2872 cm^{-1}), the C=O stretching (1721 cm^{-1}), and the additional bands of the C—C and C—O stretching (1154–1128–1066 cm^{-1}) are observed, whereas the bands of the C—H stretching (3083–3061–3027 cm^{-1}), the C=C stretching (1601 cm^{-1}), the C—C vibration (1493–1454 cm^{-1}), and the C—H bending (759–698 cm^{-1}) are related to the aromatic ring of phenyl group [53]. As shown for the previous two binders, the strong hydrolytic degradation increases the intensity of most spectral signals. The presence of new —OH groups within the molecular structure of the binder yields to the decrease of the spectral signal at 759–689 cm^{-1} of the phenyl group (aromatic C—H out of plane bending). This intensity signal decreases with the increase of relative humidity. Furthermore, a shoulder around 1670 cm^{-1} is formed. This band is assigned to the carbonyl group C=O of the formed carboxylic acids. These carboxylic groups are the result of a splitting of the lateral groups due to their oxidative decomposition. The broadening of the main carbonyl absorption at 1726 cm^{-1} may also be due to the formation of ketone and aldehyde groups which act more rapidly than the degradation of the ester groups [53]. Lastly, it is possible to observe that styrene-acrylic and acrylic samples, exposed to NO_x, show an increase of the —OH band (around 3220 cm^{-1}) at RH values of 50%, which however tends to decrease at higher RH (80%). It is due to the impact of humidity on the catalytic conversion of NO_2 on both paints. Their interaction increases with the decrease in relative humidity from 80% to 50%. It may be due to the fact that, as humidity increases, more water vapour is adsorbed

onto the surface, increasing competition for adsorption sites. Furthermore, the effect of humidity on the conversion of a pollutant also depends on its concentration. In fact, the competition for the adsorption sites between NO_2 and water vapour is already sufficient with a small amount of humidity for the generation of OH radicals. Therefore, the catalytic activity of NO_2 decreases [54].

3.3. ATR-FTIR mapping and semi-quantification of functional groups

ATR-FTIR chemical mapping is increasingly used to investigate cultural heritage materials. In fact, it was already employed as a valuable technique for analysing the distribution of pigments, additives, and binders. In recent studies, it was also applied to investigate degradation products formed on paint surfaces [55]. During this study, mapping was mainly necessary to investigate the distribution of specific degradation products on the different paint mixtures caused by the influence of each inorganic pigment. For the mapping of acrylic paints, the spectral signal of the surfactant (2895 cm^{-1}) was considered as its intensity changes with the different pigment in the mixture. In Fig. 3, the spectra of the acrylic paint samples exposed to SO_2 (Fig. 3a) and NO_x (Fig. 3b) at 80% RH are shown. Integrating the area of the selected band, and observing its distribution on the surface of the samples, it is possible to conclude that the mixture with PW6 facilitates the migration of the surfactant on the surface followed by PB29 and PB28 (exposed to SO_2), and pure binder and PB35 (exposed to NO_x). As reported in literature [56], titanium dioxide (PW6) has a strong catalytic effect and, in this case, when the water molecule comes into contact with the surface, its O atom strongly interacts with the Ti atoms present in the paint layer. In this way, H atoms trap electrons from Ti atoms and become negative. The water molecule is then adsorbed and the surfactant is more prone to migrate to the surface. The surfactant behaviour has been further investigated by semi-quantitative evaluation. It was performed on unaged, 50% and 80% RH aged samples for both corrosive gases, integrating not only the surfactant band area at 2895 cm^{-1} but also those at 1343 and 1115 cm^{-1} (Table S2). From the integration values of the three set of samples, the differences between the unaged and 50% RH aged, and between 50% and 80% RH aged were calculated (Table S3).

In Fig. S5, it is possible to confirm that the acrylic mixture with PW6 causes the most significant migration of surfactant on the surface. Furthermore, NO_x appears to have a more oxidizing effect than SO_2, confirming the previous results discussed. The mapping of the alkyd paint samples was performed by integrating the C═O carbonyl band at 1721 cm^{-1} and the C—H bond at 2926–2854 cm^{-1}. Furthermore, the degradation product bands at 1414 cm^{-1} and 1630 cm^{-1} were also considered.

In all paint mixtures, exposed to SO_2 and NO_x the distribution of these bands on the surface show already a sharp increase, after the first ageing cycle at 50% RH. Subsequently, increasing the relative humidity, this trend is only slightly increased. Generally, all paint mixtures show this behaviour. However, those with PR101 and PW6 are more prone to hydrolytic degradation (Fig. S6).

This trend is confirmed by the semi-quantitative evaluation (Fig. S5c, d) of the bands mentioned above. The degradation effects on alkyd paints are similar for both gases, as they are chemically more prone to interact with the drying oil present in the binder, influencing the oxidation process [57]. Finally, the mapping of styrene-acrylic paints was investigated by integrating the C—H bands at 2961 cm^{-1}, the C═O carbonyl band at 1725 cm^{-1}, and the OH band at 3248 cm^{-1}. The evaluation of this latter band, through chemical mapping and semi-quantification confirms the decreasing catalytic effect of NO_x with increasing of relative humidity. In Fig. S5e, f, this behaviour is particularly evident in comparison to SO_2 ageing. Therefore, the evaluation of the degradation processes of styrene-acrylic paints is the most complex, since the catalytic activity of NO_x is already activated at RH of 50%. In contrast, the deterioration action of SO_2 grows exponentially with increasing of relative humidity.

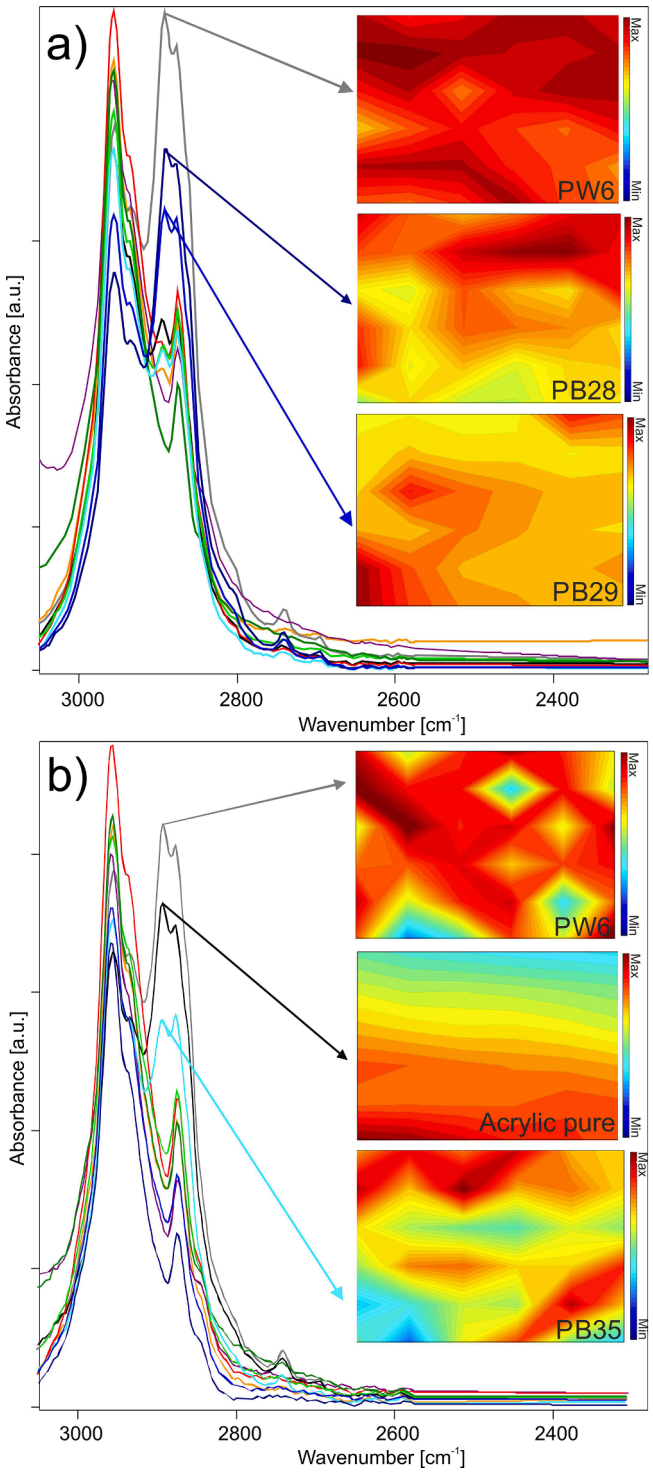

Fig. 3. ATR-FTIR chemical mapping of the surfactant distribution, after a) SO_2 and b) NO_x exposure of acrylic paint mixtures with PW6 (grey), PY37 (orange), PG50 (light green), PG18 (dark green), PB35 (cyan), PB28 (blue), PB29 (dark blue), PR101 (red), PV16 (purple), and pure binder (black).

3.4. Principal component analysis results

The score plots in Fig. 4 show the results obtained from the multivariate exploratory analysis on the paint mixtures, divided according to binder type and gas exposure. Fig. 4a reports the PC1 and PC2 score plot obtained from the spectra of the acrylic mixtures aged with SO_2. PC1 and PC2 retain 78.2% and 15.5% of explained variance, respectively, with a

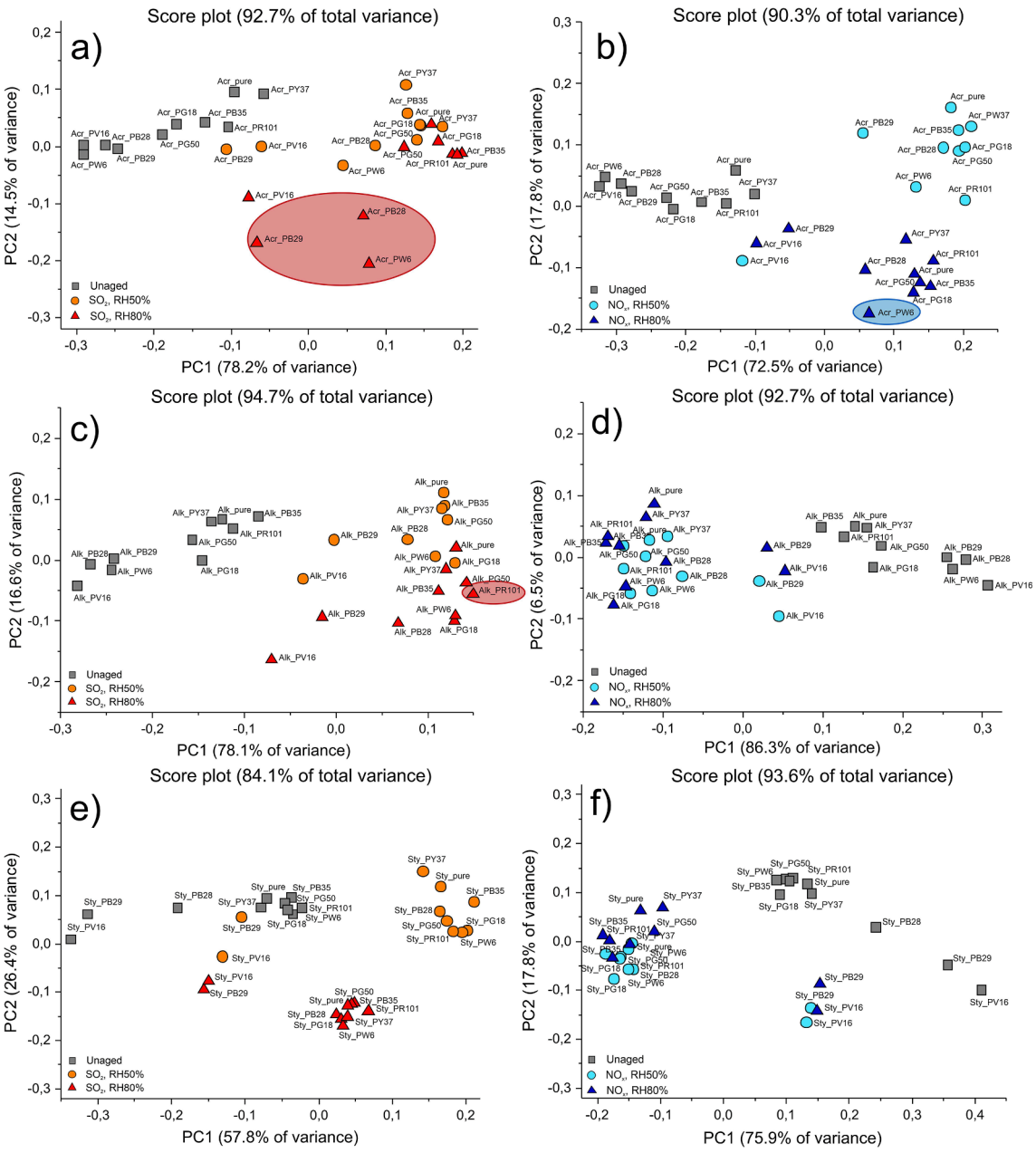

Fig. 4. PC1 and PC2 score plots of acrylic samples aged with a) SO_2 (50, 80% RH), b) NO_x (50, 80% RH); alkyd samples aged with c) SO_2 (50, 80% RH), d) NO_x (50, 80% RH); and styrene-acrylic samples aged with e) SO_2 (50, 80% RH), f) NO_x (50, 80% RH).

total of 92.7% of data variance. The cluster of unaged samples is well-differentiated from the others mainly along PC1. From the evaluation of the corresponding PC1 loading vector (Fig. S7a), this behaviour is related to the carbonyl band C═O (at 1727 cm^{-1}); therefore, this separation is given by the effect of hydrolytic degradation. Considering the aged samples, it is not possible to clearly separate the samples according to RH% values, even if the samples aged at RH% values equal to 80% tend to have higher PC1 score values than the samples aged with 50% of relative humidity. Interestingly, PC2 describes the ageing behaviour of the three mixtures prepared with PB28, PB29 and PW6 pigments and aged at 80% of relative humidity, which have negative score values along PC2. In this case, one of the more relevant spectral regions observed on the PC2 loading vector is represented by the aliphatic C—H band at 2894 cm^{-1}, assigned to the surfactant signal. This behaviour shows that the three paint mixtures appear more subject to the effects of SO_2 at high humidity, causing the greatest migration of the surfactant on the surface. The PC1 and PC2 score plot obtained from the analysis of the acrylic samples aged with NO_x is reported in Fig. 4b, PC1 and PC2 account for 72.5% and 17.8% of explained variance, respectively. Also in this case, PC1 allows separating unaged and aged samples, while PC2 allows differentiating the aged samples according to the RH% values. Considering the PC2 loading vector reported in Fig. S7b, the surfactant band at 2894 cm^{-1} has a strong influence in the separation of the set of samples aged at RH 80%. The paint mixture with PW6 pigment again shows a more deteriorating effect. Therefore, the exposure of NO_x gas results more oxidizing for acrylic paints compared to SO_2, especially at RH 80%. The PCA score plots obtained from the analysis of the alkyd mixtures aged with SO_2 and NO_x are reported in Fig. 4c and d, respectively. For both evaluations, the clusters of data are represented according to the first two principal components PC1 and PC2. Concerning SO_2 ageing, the main distinction between unaged and aged samples is described by PC1, accounting for 78.1% of data variance. The

observation of the corresponding PC1 loading vector (Fig. S7c) shows that this separation is mainly ascribable to the C═O carbonyl band at 1721 cm^{-1} and the C—H bond at 2926–2854 cm^{-1}. Furthermore, PC2 separates quite well the samples subjected to different humidity levels.

This separation is mainly ascribable to the spectral region at 2926–2854 cm^{-1} (C–H bond) influenced by the presence of water in the molecular structure. This trend allows understanding that the high humidity facilitates the hydrolysis of the bonds of the phthalate group of the binder. The consequent broadening of the band C═O (PC1) defines the mixture with PR101 as the most subject to degradation effect. Also considering NO_x ageing, PC1 allows separating unaged and aged samples and the relevant spectral bands responsible for this separation are the same as those observed for SO_2 ageing (C═O and C—H bond). However, in this case, it is not possible to easily differentiate the aged samples according to the different relative humidity values. Lastly, Fig. 4e-f show the PC1 and PC2 score plots obtained from the analysis of the styrene-acrylic mixtures, representing the 84.1% of explained variance for SO_2 aged samples, and 93.6% of explained variance for NO_x aged samples.

Concerning SO_2 ageing, the main distinction between unaged and aged samples is given by PC1 and this behavior is mainly ascribable to C═O carbonyl band at 1727 cm^{-1} (Loadings in Fig. S7e, f). Furthermore, PC2 allows separating the samples aged with SO_2 + RH80% from the other clusters; indeed, these samples show negative values of PC2 scores. Observing the corresponding PC2 score vector (Fig. 4e), the spectral region related to the C—H bond (2926–2854 cm^{-1}) has a higher relevance in defining PC2 direction. It means that, by increasing the relative humidity, the OH groups present in the artificial atmosphere are more able to have an oxidizing effect on the phenyl groups of the binder. Finally, also for NO_x ageing, the main distinction between unaged and aged is given by PC1 (Fig. 4f), whose direction is mainly influenced by the spectral regions related to C═O (1727 cm^{-1}) and C—H (2926–2854 cm^{-1}) bonds (Fig. S7f). Considering the RH% values, in this case, it is not possible to observe a clear separation between samples aged with different relative humidity levels, however, the samples processed with an RH% equal to 50% tend to be more distant from the corresponding unaged samples in the PC1 and PC2 score plot. For both gaseous exposures, both for alkyd and styrene-acrylic paints, the mixtures with PB29 and PV16 show a similar trend. They are always placed between the unaged and aged clusters, independently of the relative humidity value selected. This behaviour may be due to a lower degrading effect of corrosive agents on these two paints, leading to a lower spectral signal

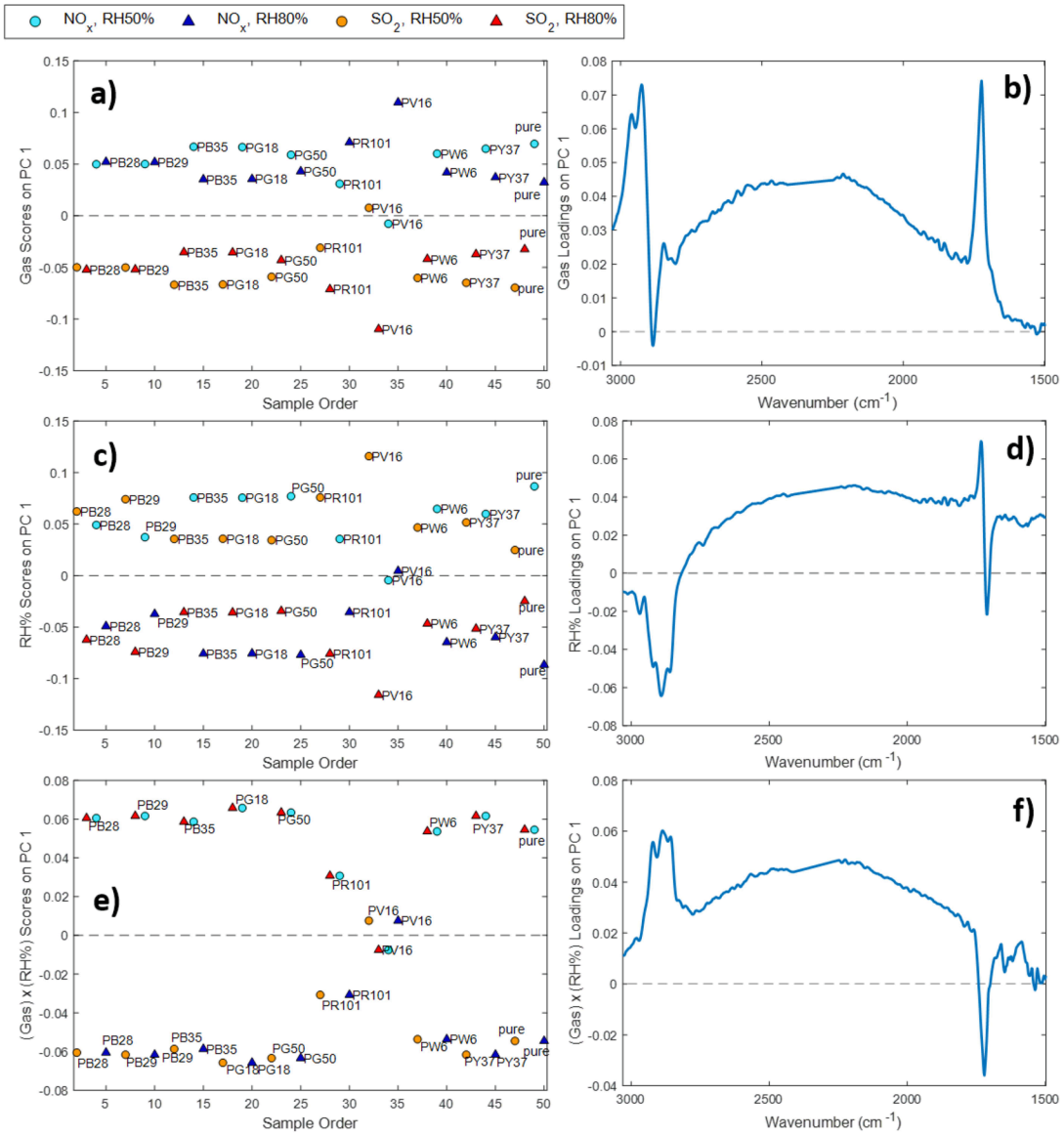

Fig. 5. ASCA results of acrylic paint samples; score and loading plots of the a-b) gas, c-d) RH%, and e-f) gas × RH% sub-models.

compared to the other paint mixtures.

3.5. ASCA results

Table S4 reports the results obtained by applying ASCA to the aged samples separated according to binder type in order to systematically evaluate the influence of individual experimental factors (pigment, gas, RH%) and their interactions (pigment × gas, pigment × RH%, gas × RH %) on the degradation process of the different paint mixtures. Generally, for all the three datasets pigment type is the factor showing the highest effect on the spectral response, accounting for more than 50% of data variance, while its interaction with gas or RH% is not significant. The investigation of the PCA sub-models related to pigment factor allowed to observe that such effect is due to the peculiar behaviour of the mixtures containing PV16 and PB29 pigments for all the three binder types, which have a lower degradation and, as a consequence, spectra with lower intensity (as previously outlined). The ASCA results obtained on the samples of acrylic paints show that RH% factor (12.88%) has a higher influence on the spectral response compared to gas factor (10.81%) or gas × RH% interaction (10.51%). Considering the score and loading plots of gas sub-model (Fig. 5a-b), the exposure to NO_x causes the greatest intensity increase of the bands at 1727 cm^{-1} (C═O bond) and 2895 cm^{-1} (PEO surfactant), and therefore a higher degradation of the sample. As far as the RH% effect is concerned, the influence of high levels of relative humidity (Fig. 5c, d) mainly affects the surfactant band at 2956–2876 cm^{-1} (C–H bond). From the evaluation of the gas × RH% interaction (Fig. 5e, f), it is possible to observe that the exposure of the paint samples to NO_x at RH 80% mainly causes the intensity increase of the band at 1721 cm^{-1}, while the exposure to SO_2 at RH 80% has a great influence on the surfactant band at 2895 cm^{-1}. Therefore, the degradation of acrylic paints is mainly caused by the exposure of NO_x to 80% RH, causing the migration of the surfactant on the surface. These results confirm the previous considerations. Regarding the ASCA results for alkyd paint samples (Table S4), gas factor (15.42%) has the stronger influence on the spectral response, followed by gas × RH% interaction (11.50%) and RH% factor (7.40%).

Compared to the results obtained with acrylic mixtures, for alkyd paint samples the effect of gas type in the degradation process is more evident. Indeed, in this case, gas factor accounts for a higher percentage of explained variance and the score plot of gas sub-model shows a clear separation between the samples aged with the two gases (Fig. S8a). Considering the loading vector of gas sub-model (Fig. S8b), it is possible to observe that NOx degradation determines a higher increase of the spectral bands related to C═O (1721 cm^{-1}) and C–H bonds (2956–2876 cm^{-1}). Besides, the spectra of the sample aged with NOx have a peculiar band at about 1630 cm-1, which can be ascribable to the -O-NO_2 degradation product. For alkyd paints, RH% factor has a lower effect compared to gas × RH% interaction, therefore the degradation of the aged samples (ascribable only to the different humidity levels) is less marked than the degradation due to the combination of gas and RH%. Considering the results of gas × RH% sub-model (Fig. S8e, f), the samples aged with NOx and RH% equal to 80% are characterized by a higher increase in the C═O band at 1721 cm^{-1}, while the spectral region centred at about 2880 cm^{-1} is mainly influenced by SO_2 ageing with RH % values equal to 80%. Considering the ASCA results reported in Table S4, for styrene-acrylic paint samples the degradation process is more influenced by gas × RH% interaction (16.45%) than gas (13.11%) and RH% (9.02%) factors taken individually. Therefore, the degradation process of these paints depends on the specific combination between gas type and RH% level. Similarly, to what observed for the other binders, NO_x generally determines a higher increase of the two characteristic bands at 1727 cm^{-1} and 2956–2930 cm^{-1} (Fig. S9a, b). Furthermore, the score plot of gas sub-model shows a quite marked separation between the samples according to gas type, as previously observed for alkyd paints. Considering gas × RH% sub-model (Fig. S9e, f), the different combinations of the two factors have a different deteriorating effect. In fact, the peak centred at 1740 cm^{-1} has a higher intensity for the samples aged with NO_x and RH% equal to 80% and for the samples aged with SO_2 and RH% equal to 50%. Conversely, the degradation process observable in the spectral region centred at 2915–2880 cm^{-1} is more influenced by the exposure to SO_2 and RH% equal to 80% or to NO_x and RH% equal to 50%. Summarizing the ASCA results related the effect of the gas, RH%, and their two-way interaction on the mixtures prepared with the three binder types, it is possible to observe that the exposure to NO_x generally has a more degrading effect on the paint samples. In particular, alkyd mixtures are more subjected to the influence of the gas type. The effect of the different levels of RH% is mainly observable in the spectral region at 2915–2880 cm^{-1}, and the ageing process of acrylic paints is slightly more influenced by relative humidity. Furthermore, ASCA results also showed that the interaction between gas and RH% plays an important role in the degradation of the samples, in particular for styrene-acrylic mixtures.

4. Conclusion

During this study, an accelerated gas ageing on modern paint samples was performed trying to simulate real outdoor environmental conditions. In particular, sulphur dioxide (SO_2) and nitrogen oxide (NO_x) were used and mixed with different relative humidity content (50% and 80% RH) for a total of 168 h gas exposure. The paint samples are mixtures of three different binding media (acrylic, alkyd, and styrene-acrylic) with various inorganic pigments. After ageing, the samples were analyzed by various analytical techniques whose results are listed as follows: morphological observations by 3D microscope seemed to show the most significant degradation effects on acrylic paints with the consequent surface migration of the surfactant. The different morphological changes deriving from the exposure of the two gases were studied by analyzing the depth and roughness profile showing a higher oxidative behaviour with NO_x. From the qualitative and semi-quantitative ATR-FTIR analysis, the various binders and ageing conditions showed different results: the acrylic paints are more subjected to NO_x degradation (surfactant migration). Moreover, the semi-quantitative evaluation and chemical mapping showed that paints with PW6, PB29, and PB28 favour this deteriorating behaviour. Alkyd paints show similar degradation levels when exposed to pollutant gases. The main degradation reaction is the hydrolysis of the phthalic component in the binder, although it seems favoured by the interaction with NO_x, while SO_2 tends to interact more with the drying oil. The pigments that favour these reactions are PW6 and PR101. Finally, styrene-acrylic paints are more sensitive to the interaction gas-relative humidity, showing two different degradation behaviours. The multivariate methods used (PCA and ASCA) confirmed both the results previously obtained and brought more information useful for understanding the different chemical mechanisms between materials and polluting agents. By PCA, it was possible to understand that, in all paints, the functional groups C—H and C═O are the most subject to degradation. Furthermore, it confirmed that this effect is enhanced with certain pigments. The influence that different pigments have on the overall degradation of the binders was confirmed by ASCA. In addition, ASCA results show that the three binders are differently subject to degradation conditions. In fact, RH% has more influence on acrylic paints, than different gases on alkyd paints, and the gas × RH% combination on styrene-acrylic paints. Generally, from all the assessments performed, NO_x revealed the most significant oxidizing effect on the paints. These results are relevant as the outdoor artworks are more and more affected by environmental degradation, due to the continuous climatic changes. Understanding their deterioration reactions caused by the interaction with pollutant gases, it is essential to provide appropriate suggestions for their preservation. Considering that samples show different degradation behaviours depending on the chosen degrading agent, prevention methods should be selected according to the type of binder and the environment (indoor or outdoor) in which the artwork is

exposed or stored [58,59]. In order to obtain extensive and more detailed knowledge about artificial gas aging, future experiments will be considered. As mentioned in the introduction, the effect of ozone and particulate matter also significantly influences the stability of artworks. Therefore, their chemical-physical evaluation and correlation with the pollutants presented in this study remain a subject for future study. Another consideration for future study is the cross evaluation of pollutants and parallel aging tests (accelerated and natural). These two additional approaches will provide additional information about the stability of polymer films and the oxidising effect that each gas has with different art materials.

CRediT authorship contribution statement

Laura Pagnin: Conceptualization, Investigation, Writing - original draft, Methodology. **Rosalba Calvini:** Software, Validation. **Rita Wiesinger:** Supervision, Conceptualization. **Manfred Schreiner:** Supervision, Writing - review & editing.

Declaration of Competing Interest

The authors declare that they have no known competing financial interests or personal relationships that could have appeared to influence the work reported in this paper.

Acknowledgements

We gratefully acknowledge MSc. Laura Rabbachin (Academy of Fine Arts Vienna) for the chemical mappings carried out during this study, and MSc. Luca Guarnieri (University of Cardiff) for the support and constructive conversations during the chemical evaluation of ATR-FTIR spectra.

Availability of data and materials

Additional data about 3D images, FTIR results, and multivariate analysis are available upon request.

Funding

This research did not receive any specific grant from funding agencies in the public, commercial, or not-for-profit sectors.

Appendix A. Supplementary data

Supplementary data to this article can be found online at https://doi.org/10.1016/j.microc.2021.106087.

References

[1] Hamilton R, Kucera V, Tidblad J, Watt J. The Effects of Air Pollution on Cultural Heritage. 2009.
[2] 2. Phipps PBP, Rice DW. The Role of Water in Atmospheric Corrosion. In: Corrosion Chemistry. 1979:235–61.
[3] Cass GR, Druzik JR, et al. Protection of Works of Art From Atmospheric Ozone. The Getty Conservation Institute, 1989.
[4] F.C. Izzo, E. Balliana, F. Pinton, E. Zendri, A preliminary study of the composition of commercial oil, acrylic and vinyl paints and their behaviour after accelerated ageing conditions, Conserv. Sci. Cult. Herit. 14 (1) (2014) 353–369.
[5] Health effects of air Pollution with Particulate Matter, Ozone and Nitrogen Dioxide. World Heal Organ. 2003;EUR/03/504:95–113.
[6] J. Grau-Bové, B. Budič, I.K. Cigić, D. Thickett, S. Signorello, M. Strlič, The effect of particulate matter on paper degradation, Herit. Sci. 4 (1) (2016) 4–11.
[7] J. Tidblad, V. Kucera, M. Ferm, K. Kreislova, S. Brüggerhoff, S. Doytchinov, et al., Effects of air pollution on materials and cultural heritage: ICP materials celebrates 25 years of research, Int. J. Corros. 2012 (2012) 2005–2006.
[8] G. Ranalli, M. Matteini, I. Tosini, E. Zanardini, C. Sorlini, Bioremediation of cultural heritage: removal of sulphates, nitrates and organic substances, Of Microbes Art. 2000 (2000) 231–245.
[9] J. Aramendia, L. Gómez-Nubla, K. Castro, J.M. Madariaga, Spectroscopic speciation and thermodynamic modeling to explain the degradation of weathering steel surfaces in SO2 rich urban atmospheres, Microchem. J. 115 (2014) 138–145.
[10] M.P. Colombini, F. Modugno, R. Fuoco, A. Tognazzi, A GC-MS study on the deterioration of lipidic paint binders, Microchem. J. 73 (1–2) (2002) 175–185.
[11] W. Funke, H. Haagen, Influence of sulfur dioxide on organic coatings, ACS Symp. Ser. 309–15 (1983).
[12] L. Dulog, The role of sulfur dioxide and nitrogen dioxide on the degradation of polymers, Angew. Makromol Chem. 252 (1997) 1–10.
[13] V. Gomes, A. Dionísio, Pozo-Antonio J. Santiago, The influence of the SO2 ageing on the graffiti cleaning effectiveness with chemical procedures on a granite substrate, Sci. Total Environ. 625 (2018) 233–245.
[14] Camuffo D, Fernicola V, Bertolin C. Basic Environmental Mechanisms Affecting Cultural Heritage, 2010.
[15] F. De Santis, V. Di Palo, I. Allegrini, Determination of some atmospheric pollutants inside a museum: relationship with the concentration outside, Sci. Total Environ. 127 (3) (1992) 211–223.
[16] Learner TJS. Analysis of Modern Paints. The Getty Conservation Institute; 2005.
[17] NIIR Board of Consultants & Engineers. Modern Technology of Synthetic Resins & Their Applications. Asia Pacific Business Press Inc. 2018.
[18] Learner TJS, Smithen P, Krueger JW, Schilling MR. Modern Paints Uncovered. The Getty Conservation Institute; 2007.
[19] L. Feller Artists' Pigments A Handbook of Their History and Characteristics. 1986.
[20] A. Roy Artists' Pigments A Handbook of Their History and Characteristics. 1993.
[21] Fitzhugh EW. Artists' Pigments. A Handbook of Their History and Characteristics. 1997.
[22] B. Berrie Artists' Pigments A Handbook of Their History and Characteristics. 2007.
[23] G. Musumarra, M. Fichera, Chemometrics and cultural heritage, Chemometr. Intell. Labor. Syst. 44 (1–2) (1998) 363–372.
[24] G. Capobianco, M.P. Bracciale, D. Sali, F. Sbardella, P. Belloni, G. Bonifazi, M. C. Guidi, et al., Chemometrics approach to FT-IR hyperspectral imaging analysis of degradation products in artwork cross-section, Microchem. J. 132 (2017) 69–76.
[25] G. Abdel-Maksoud, M. Ibrahim, Y.M. Issa, M. Magdy, Investigation of painting technique of coptic icon by integrated analytical methods: imaging, spectroscopic and chemometric methods, J. Archaeol. Sci. Rep. 29 (2020).
[26] L. Pagnin, R. Calvini, R. Wiesinger, J. Weber, M. Schreiner, Photodegradation kinetics of alkyd paints: the influence of varying amounts of inorganic pigments on the stability of the synthetic binder, Front. Mater. 7 (2020) 1–15.
[27] E. Marengo, M.C. Liparota, E. Robotti, M. Bobba, Monitoring of paintings under exposure to UV light by ATR-FT-IR spectroscopy and multivariate control charts, Vibrat. Spectrosc. 40 (2) (2006) 225–234.
[28] G. Bonifazi, G. Capobianco, C. Pelosi, S. Serranti, Hyperspectral imaging as powerful technique for investigating the stability of painting samples, J. Imag. 5 (1) (2019) 8.
[29] C. Pelosi, G. Capobianco, G. Agresti, G. Bonifazi, F. Morresi, S. Rossi, S. Serranti, et al., A methodological approach to study the stability of selected watercolours for painting reintegration, through reflectance spectrophotometry, Fourier transform infrared spectroscopy and hyperspectral imaging, Spectrochim. Acta A Mol. Biomol. Spectrosc. 198 (2018) 92–106.
[30] L. Ortiz-Herrero, I. Cardaba, S. Setien, L. Bartolomé, M.L. Alonso, M.I. Maguregui, OPLS multivariate regression of FTIR-ATR spectra of acrylic paints for age estimation in contemporary artworks, Talanta 205 (2019).
[31] Berni A, Mennig M, Schmidt H. Doctor Blade. Sol-Gel Technologies for Glass Producers and Users. 2004:89–92.
[32] R. Wiesinger, M. Schreiner, C. Kleber, Investigations of the interactions of CO2, O3 and UV light with silver surfaces by in situ IRRAS/QCM and ex situ TOF-SIMS, Appl. Surf. Sci. 256 (9) (2010) 2735–2741.
[33] 33. Available from https://www.eea.europa.eu/.
[34] P.M. Carmona-Quiroga, R.M.J. Jacobs, S. Martínez-Ramírez, H.A. Viles, Durability of anti-graffiti coatings on stone: natural vs accelerated weathering, PLoS ONE 12 (2) (2017) 1–18.
[35] R. Wiesinger, L. Pagnin, M. Anghelone, L.M. Moretto, E.F. Orsega, M. Schreiner, Pigment and binder concentrations in modern paint samples determined by IR and raman spectroscopy, Angew. Chem. Int. Ed. 57 (25) (2018) 7401–7407.
[36] A. Sarmiento, M. Pérez-Alonso, M. Olivares, K. Castro, I. Martínez-Arkarazo, L. A. Fernández, et al., Classification and identification of organic binding media in artworks by means of Fourier transform infrared spectroscopy and principal component analysis, Anal. Bioanal. Chem. 399 (10) (2011) 3601–3611.
[37] L. Pagnin, L. Brunnbauer, R. Wiesinger, A. Limbeck, M. Schreiner, Multivariate analysis and laser-induced breakdown spectroscopy (LIBS): a new approach for the spatially resolved classification of modern art materials, Anal. Bioanal Chem. 412 (2020) 3187–3198.
[38] J.J. Jansen, H.C.J. Hoefsloot, J. Van Der Greef, M.E. Timmerman, J.A. Westerhuis, A.K. Smilde, ASCA: analysis of multivariate data obtained from an experimental design, J. Chemom. 19 (9) (2005) 469–481.
[39] G. Zwanenburg, H.C.J. Hoefsloot, J.A. Westerhuis, J.J. Jansen, A.K. Smilde, ANOVA–principal component analysis and ANOVA–simultaneous component analysis: a comparison, J. Chemom. 25 (10) (2011) 561–567.
[40] A. Savitzky, M.J.E. Golay, Smoothing and differentiation of data by simplified least squares procedures, Anal Chem. 36 (8) (1964) 1639–1643.
[41] 41. Leardi R, Melzo C, Polotti G. Chemometric agile software (CAT). Gruppo di chemiometria; Available from: http://gruppochemiometria.it/index.php/software.
[42] S. Digney-Peer, A. Bumstock, T. Leamer, H. Khanjian, F. Hoogland, J. Boon, The migration of surfactants in acrylic emulsion paint films, Stud. Conserv. 49 (2) (2004) 202–207.

[43] M. Anghelone, V. Stoytschew, D. Jembrih-Simbürger, M. Schreiner, Spectroscopic methods for the identification and photostability study of red synthetic organic pigments in alkyd and acrylic paints, Microchem. J. 139 (2018) 155–163.
[44] B. Ormsby, G. Foster, T. Learner, S. Ritchie, M. Schilling, Improved controlled relative humidity dynamic mechanical analysis of artists' acrylic emulsion paints: Part II. General properties and accelerated ageing, J. Therm. Anal. Calorim. 90 (2) (2007) 503–508.
[45] B. Ormsby, T. Learner, M. Schilling, J. Druzik, H. Khanjian, G. Foster, et al., The effects of surface cleaning on acrylic emulsion paintings: a preliminary investigation, Tate Pap. 6 (2006) 1–14.
[46] E. Jablonski, T. Learner, J. Hayes, M. Golden, Conservation concerns for acrylic emulsion paints, Stud Conserv. 48 (1) (2003) 3–12.
[47] J.N.B. Bell, M. Treshow, Air Pollution and Plant Life, Wiley, 2002.
[48] E. Davydov, I. Gaponova, G. Pariiskii, T. Pokholok, R. Academy, Reactivity of polymers on exposure to nitrogen oxide, Chem. Chem. Technol. 4 (4) (2010).
[49] M. Anghelone, D. Jembrih-Simbürger, M. Schreiner, Influence of phthalocyanine pigments on the photo-degradation of alkyd artists' paints under different conditions of artificial solar radiation, Polym. Degrad Stab. 134 (2016) 157–168.
[50] F.X. Perrin, M. Irigoyen, E. Aragon, J.L. Vernet, Evaluation of accelerated weathering tests for three paint systems: a comparative study of their aging behaviour, Polym. Degrad. Stab. 72 (1) (2001) 115–124.
[51] W.H. Simendinger, C.M. Balik, Chemical reactions of sulfur dioxide and oxygen with unsaturated drying oils and an alkyd paint, J. Coatings Technol. 66 (837) (1994) 39–45.
[52] Socrates G. Infrared and Raman characteristic group frequencies. Tables and charts. Journal of Raman Spectroscopy. 2001.
[53] Z.E. Papliaka, K.S. Andrikopoulos, E.A. Varella, Study of the stability of a series of synthetic colorants applied with styrene-acrylic copolymer, widely used in contemporary paintings, concerning the effects of accelerated ageing, J. Cult. Herit. 11 (4) (2010) 381–391.
[54] T. Maggos, J.G. Bartzis, P. Leva, D. Kotzias, Application of photocatalytic technology for NOx removal, Appl. Phys. A Mater. Sci. Process. 89 (1) (2007) 81–84.
[55] E.J. Henderson, K. Helwig, S. Read, S.M. Rosendahl, Infrared chemical mapping of degradation products in cross-sections from paintings and painted objects, Herit. Sci. 7 (1) (2019).
[56] E. Rangel, G. Ruiz-Chavarria, L.F. Magana, Water molecule adsorption on a titanium-graphene system with high metal coverage, Carbon N. Y. 47 (2) (2009) 531–533.
[57] Spence JW, Haynie FH. Paint Technology and Air Pollution: A Survey and Economic Assessment. 1972.
[58] Pollution Prevention in the Paints and Coatings Industry. Agency USEP. 1996.
[59] C.M. Grzywacz, Monitoring for gaseous pollutants in museum environments, Tools Conserv. (2006) 1–76.